Annals of Nuclear Medicine Vol. 13, No. 2, 101–107, 1999

Effect of tracer metabolism on PET measurement of [^{11}C]pyrilamine binding to histamine H_1 receptors

Sang Eun KIM,* Zsolt SZABO,** Chie SEKI,** Hayden T. RAVERT,**
Ursula SCHEFFEL,** Robert F. DANNALS** and Henry N. WAGNER, Jr.**

*Department of Nuclear Medicine, Samsung Medical Center, Sungkyunkwan University School of Medicine, Seoul, Korea
**Divisions of Nuclear Medicine and Radiation Health Sciences,
The Johns Hopkins Medical Institutions, Baltimore, Maryland, U.S.A.

The present study was carried out to investigate the time course of [^{11}C]pyrilamine metabolism and the degree of entry of metabolites into the brain. PET studies were performed in seven healthy volunteers and arterial plasma concentrations of [^{11}C]pyrilamine and its labeled metabolites were determined. After intravenous injection, [^{11}C]pyrilamine metabolized gradually in the human body, with less than 10% of plasma activity being original radioligand at 60 min. Tracer metabolism markedly affected the input function and the calculated impulse response function of the brain. Rat experiments demonstrated that although metabolites of [^{11}C]pyrilamine might enter the brain, they were not retained for prolonged periods of time. At 30–90 min after injection of [^{11}C]pyrilamine, less than 1% of the radioactivity in the brain was originating from metabolites of [^{11}C]pyrilamine. Based on the rat data, the contribution of ^{11}C-labeled metabolites to total [^{11}C]pyrilamine radioactivity in the human brain was estimated and found to be negligible. These results suggest that the metabolites of [^{11}C]pyrilamine do not accumulate within the cerebral extravascular space and that there is minimal metabolism of [^{11}C]pyrilamine by brain tissue itself. Therefore, [^{11}C]pyrilamine metabolites can be neglected in kinetic analysis, using either a compartmental or a noncompartmental model, of the [^{11}C]pyrilamine binding to histamine H_1 receptors.

Key words: histamine H_1 receptor, [^{11}C]pyrilamine, tracer metabolism, positron emission tomography

INTRODUCTION

HISTAMINE has been suggested as one of the principal neurotransmitters regulating alertness.[1,2] In addition to their involvement in the sleep/wake cycle, histamine H_1 receptors have been implicated in the mediation of many other behavioral processes, such as vestibular function,[3] neuroendocrine control,[4] cardiovascular control,[5] thermoregulation,[6] feeding behavior,[7] stress reaction and stress analgesia.[5] The distribution of H_1 receptors also implicates their involvement in limbic functions, such as emotion, learning, sexuality and memory.[8,9]

The antihistaminic drug pyrilamine (also known as mepyramine) binds selectively to histamine H_1 receptors and has been used to probe histamine H_1 receptors in *in vitro* and *in vivo* experiments.[10–13] Recently, pyrilamine has been labeled with the positron emitter carbon-11 and used for mapping of the histamine H_1 receptors in the human brain by positron emission tomography (PET).[14–16]

To obtain parameters of ligand-receptor interactions from PET data one has to take into account not only the blood-brain transport of ligand, ligand binding to receptors, and nonspecific binding, but also the transformation of the drug in the body. Correcting the arterial plasma activity (the input function) for the presence of drug

Received November 30, 1998, revision accepted February 15, 1999.

For reprint contact: Sang Eun Kim, M.D., Department of Nuclear Medicine, Samsung Medical Center, Sungkyunkwan University School of Medicine, 50 Ilwon-dong, Kangnam-ku, Seoul 135–710, KOREA.
E-mail: sekim@smc.samsung.co.kr

metabolites is of great importance in modeling and quantifying ligand-receptor kinetics.[17,18] Modification of the input function may not be sufficient to improve the performance of a tracer kinetic model if a labeled metabolite has a high extraction fraction so that it too would be distributed throughout the brain in a manner dependent upon regional blood flow and brain permeability.[17] Another important factor for monitoring receptor binding is whether the ligand bound to receptor sites undergoes further metabolism (i.e., metabolic stability).[19] Therefore, to measure ligand-receptor interactions *in vivo*, knowledge of the kinetics of drug metabolites both in plasma and brain is essential.

Investigations with [^{3}H]pyrilamine have shown significant metabolism of this ligand in guinea pigs.[20] The present study was designed to determine the degree and time course of [^{11}C]pyrilamine metabolism in humans and their effect on PET measurements of receptor binding. Since in humans it is not possible to determine the transfer of metabolites into the brain unless the nature of the metabolites is known, they are radiolabeled and permission is obtained to administer them parenterally, data from rodent studies have to suffice to estimate the contribution of metabolites to the total brain radioactivity. Therefore, investigations in rats were conducted with [^{11}C]pyrilamine to determine the degree to which metabolites are transferred into or generated within the brain. The investigation reported here describes 1) the entry and generation of [^{11}C]pyrilamine metabolites in the rat brain; 2) the measurement of ^{11}C-labeled metabolites in human plasma after injection of [^{11}C]pyrilamine; 3) the effect of plasma metabolites on the blood input function and the brain impulse response function; and 4) the estimation of the effect of [^{11}C]pyrilamine metabolites entering the human brain on PET measurements of ligand-H_1 receptor interactions.

MATERIALS AND METHODS

PET studies and plasma metabolite analysis in humans

Seven healthy males (ages 20–36 yr) with no history of ingestion of antihistaminics or other drugs and no history of psychiatric or neurological disorders were recruited. Informed consent was obtained in agreement with the Institutional Review Board guidelines.

Carbon-11-pyrilamine synthesis involved the *N*-alkylation of the nor-methyl precursor with ^{11}C-labeled methyl iodide obtained from high specific activity ^{11}C-labeled carbon dioxide produced in a Scanditronix AB RNP-16 biomedical cyclotron, as previously described.[13]

Approximately 740 MBq (20 mCi) (average 4.5 μg) of [^{11}C]pyrilamine (specific activity 1417 ± 500 mCi/μmol) was administered intravenously as a bolus with a 5-sec injection duration. PET studies were done by means of a NeuroECAT scanner with an in-plane resolution of 8 mm. PET data were acquired beginning 30 sec (the time of arrival of significant radioactivity in the brain) after [^{11}C]pyrilamine administration according to the following protocol: three 1 min scans, three 2 min scans, three 5 min scans, three 10 min scans and one 20 min scan. A 10-min transmission scan with a ^{68}Ge source was done prior to the study for subsequent attenuation correction. PET data were used to calculate the impulse response function by deconvolution analysis (see below). A radial artery catheter was placed in order to collect blood samples to determine the kinetics of total plasma radioactivity and the fraction of the total arterial radioactivity represented by unmetabolized [^{11}C]pyrilamine. Total plasma radioactivity was obtained according to the following sampling protocol: 5 sec intervals for the first 2 min, 1 min intervals up to 10 min, 2 min intervals up to 20 min, and 5–15 min intervals up to 90 min postinjection. Arterial samples were also collected for determination of plasma metabolites by high performance liquid chromatography (HPLC) at 2, 5, 10, 20 and 60 min after tracer injection.

Samples for HPLC metabolite analyses were obtained by the following procedure. C-18 SEP-PAKs (Waters Associates, Milford, MA, U.S.A.) were activated with 5 m*l* of methanol and subsequently flushed with 5 m*l* of HPLC grade water. Plasma was isolated from 10 m*l* blood samples collected in heparinized tubes, passed slowly through the SEP-PAK, and washed with 5 m*l* of HPLC grade water to remove residual proteins. The radioactivity was then eluted off the SEP-PAK with five 1 m*l* fractions of methanol. The radioactivity in the 5 fractions and the SEP-PAK was counted. The first and second methanol fractions were pooled, and HPLC analysis performed. More than 90% of the radioactivity on the SEP-PAKs was eluted by this procedure. All separation procedures were performed with ice-cold solutions and materials. Control studies in which [^{11}C]pyrilamine was added directly to blood samples demonstrated that no metabolism or degradation occurred during the period necessary to complete the above procedure.

Two m*l* of the methanol solution containing the isolated plasma radioactivity was injected onto a C-18 reverse phase analytical column (Alltech Associates, Deerfield, IL, U.S.A., 4.6 mm × 250 mm, particle size 10 μm). All separations were performed with a vacuum-degassed mobile phase consisting of 40/60 acetonitrile/water buffered with 0.1 M ammonium formate at a flow rate of 3 m*l*/min. The HPLC eluent passed through a UV detector and subsequently through a 1 m*l* loop positioned between two opposing 5 in. NaI(Tl) detectors that were peaked to detect 511 keV photons in a singles mode. The ratemeter signal was fed to a Rainin Dynamax dual channel control/interface module with an Apple Macintosh computer and the area under each radioactive peak was calculated by means of the Dynamax software package. Peaks were identified by comparing the retention times and ultraviolet absorption ratios of the eluates with those of authentic samples (pyrilamine and *N*-desmethylpyril-

amine). The area of each peak was decay corrected to the time of sample injection and from these data the percent of the total activity represented by unchanged [^{11}C]pyrilamine was determined.

The measured metabolite percentages were interpolated linearly and multiplied by the total plasma activity to obtain the metabolite-corrected plasma time-activity curve. Details of the PET imaging studies are published elsewhere.[16] For the purpose of this work time-activity curves from regions of the frontal cortex were calculated. To examine the effect of plasma metabolites on the brain impulse response function, the impulse response functions for [^{11}C]pyrilamine in the human brain were deduced and compared by deconvolving both the metabolite-corrected and uncorrected input functions from the measured brain time-activity curve[21,22] with the MATLAB™ software package (The MathWorks Inc., Natick, MA, U.S.A.). Deconvolution was accomplished by singular value decomposition, a technique based on the matrix formulation of the convolution integral.[23] The impulse response function was calculated based on the assumption that the kinetics of [^{11}C]pyrilamine are linear and stationary.

Uptake of [^{11}C]pyrilamine and labeled metabolites in rat brain

Male Sprague-Dawley rats (Charles River Laboratories, Wilmington, MA, U.S.A.), weighing between 172 and 258 g, were used. To determine the entry of [^{11}C]pyrilamine metabolites into the brain, 740–1110 MBq (20–30 mCi) (5.0–10.9 μg) of [^{11}C]pyrilamine in a volume of 1 m*l* of saline was injected intravenously via a tail vein. At 30 min postinjection, the animals were killed by decapitation, and the blood was collected. The blood was promptly centrifuged and the plasma was stored on ice. The plasma (1.8–3.0 m*l*) was injected into a second set of rats which were then sacrificed to study the kinetics of the metabolites at 5 (n = 1), 30 (n = 2), and 60 min (n = 2) postinjection. A portion of the plasma was used for determination of [^{11}C]pyrilamine metabolites by HPLC analysis as described above. Plasma HPLC analysis showed that the majority of the radioactivity (70–100%) belonged to ^{11}C-labeled metabolites. The tissue radioactivity (see below) was corrected for unmetabolized [^{11}C]pyrilamine as determined by HPLC. For pyrilamine distribution, rats were injected intravenously via a tail vein with 37–111 MBq (1–3 mCi) (1.3–10.9 μg) of [^{11}C]pyrilamine in 1 m*l* of saline, and then sacrificed at selected times [5 (n = 2), 30 (n = 3), and 60 min (n = 3)]. The brain was removed from the skull and the cerebrum (whole brain less the cerebellum) dissected. The tissue and plasma samples were weighed and their radioactivity content measured in an automated gamma counter (1282 Compugamma CS, Pharmacia/LKB Nuclear Inc., Gaithersburg, MD, U.S.A.). Aliquots of the injected tracer were counted along with the samples and served as

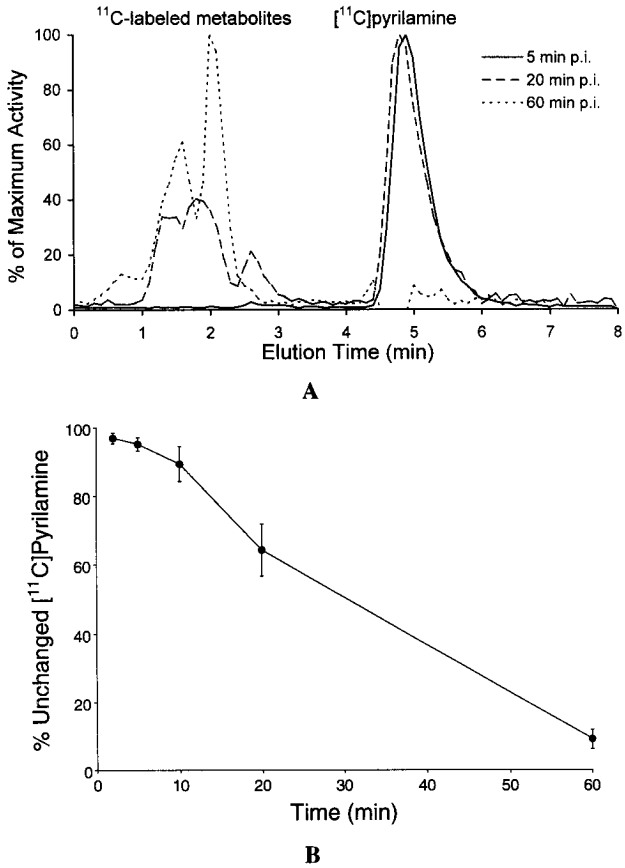

Fig. 1 A) HPLC chromatograms of human arterial plasma samples obtained at 5, 20, and 60 min after injection of [^{11}C]pyrilamine. B) Time course of [^{11}C]pyrilamine metabolism in human plasma. Data are means ± SEM.

standards for the calculation of percent injected dose per gram tissue (%ID/g). Since capillaries contain metabolized as well as unmetabolized pyrilamine, the volume of blood within the tissue contributes to the measured count rate in proportion to the total count rate for whole blood. We therefore corrected the brain radioactivity for cerebral blood volume based on the ^{99m}Tc-human serum albumin distribution.[24]

Analysis of labeled metabolites in rat brain

The chemical identification of the radioactivity detected in the brain after the administration of [^{11}C]pyrilamine was carried out in rats. Rats were injected with 74–370 MBq (2–10 mCi) (1.9–10.9 μg) of [^{11}C]pyrilamine and killed by decapitation at 30 (n = 2), 60 (n = 2), and 90 min (n = 2) postinjection. The brains were rapidly removed and homogenized with a Polytron (Brinkman) in 5 m*l* of ice-cold methanol. The homogenate was centrifuged at 50,000 *g* for 10 min. The pellet and the supernatant were separated and the respective radioactivity concentrations determined in a gamma counter. Over 85% of the radioactivity was found in the supernatant under these extraction conditions. Two m*l* of supernatant was then passed

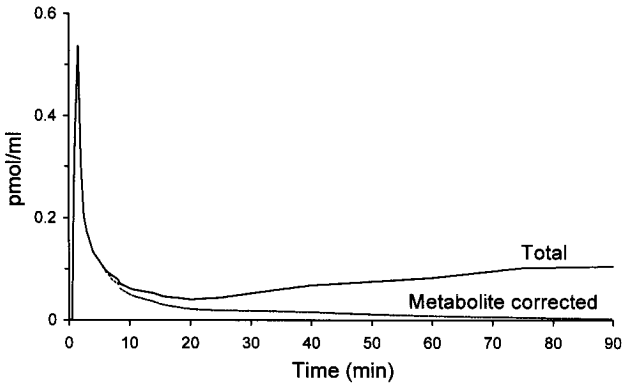

Fig. 2 Kinetics of total arterial plasma activity and unmetabolized [^{11}C]pyrilamine in one subject.

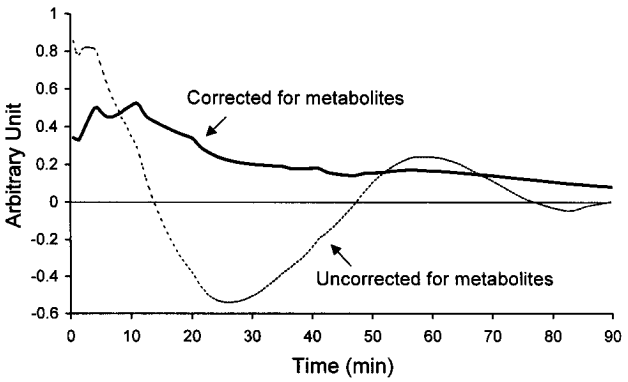

Fig. 3 Impulse response functions for [^{11}C]pyrilamine in human brain, obtained by deconvolving the measured brain time-activity curve with and without correction of the input function for labeled metabolites.

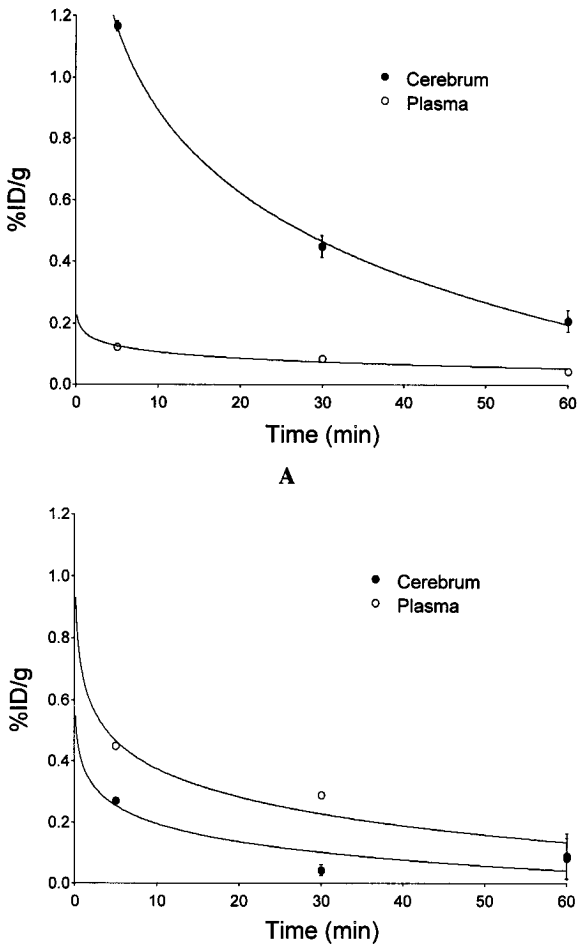

Fig. 4 Time-activity curves for [^{11}C]pyrilamine (A) and its labeled metabolites (B) in rat brain and plasma. Data are means ± SD.

through an Acro LC 13 filter and analyzed by HPLC under the same conditions as for the human plasma samples.

Estimation of labeled metabolite uptake in human brain

For the estimation of labeled metabolite uptake in human brain, we assumed that 1) plasma metabolites of [^{11}C]pyrilamine in humans are identical with those in rats, 2) blood-brain permeability in humans to [^{11}C]pyrilamine and its labeled metabolites is similar to that in rats, and 3) the initial uptake ratio of [^{11}C]pyrilamine to labeled metabolites and clearance rate for the metabolites are similar in both human and rat brains. On these assumptions, the time-activity curve representing response to injecting 100% metabolized tracer was estimated in human brain by using the data from the rat experiments and the human PET studies.

RESULTS

Analysis of human plasma metabolites by HPLC

[^{11}C]pyrilamine was metabolized in the human body, with the appearance of metabolites on HPLC analysis (Fig. 1A). Inspection of the HPLC chromatograms demonstrated that the labeled metabolites of [^{11}C]pyrilamine migrated as significantly more polar substances on the C-18 column than [^{11}C]pyrilamine itself. The time course of [^{11}C]pyrilamine metabolism is shown in Fig. 1B. Approximately 90% of the plasma radioactivity was recovered as unchanged radioligand at 10 min postinjection. Subsequently, the fraction of unmetabolized [^{11}C]pyrilamine decreased exponentially to less than 10% at 60 min postinjection.

An example of the measured plasma radioactivity and the corresponding metabolite-corrected curve is shown in Fig. 2. Whereas the total plasma radioactivity increased gradually from 20–90 min after injection, the concentration of unmetabolized [^{11}C]pyrilamine decreased continuously during this time interval. The same pattern was observed in other individuals.

The impulse response function for [^{11}C]pyrilamine in human brain was obtained by deconvolving the brain

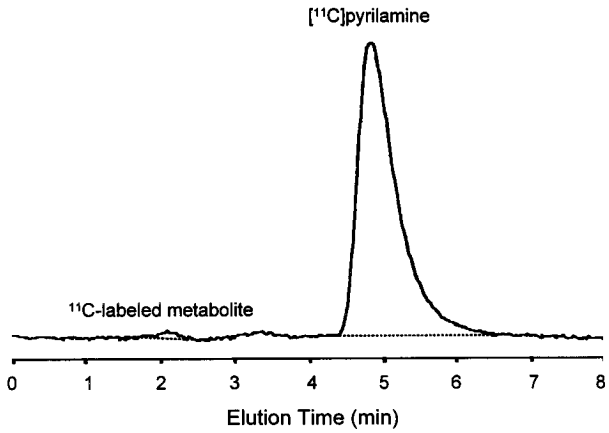

Fig. 5 HPLC chromatogram of rat brain homogenate at 30 min after injection of [^{11}C]pyrilamine, showing that less than 1% of the total radioactivity was originating from metabolites of [^{11}C]pyrilamine. HPLC of rat brain homogenates at 60 and 90 min after [^{11}C]pyrilamine injection showed a similar finding.

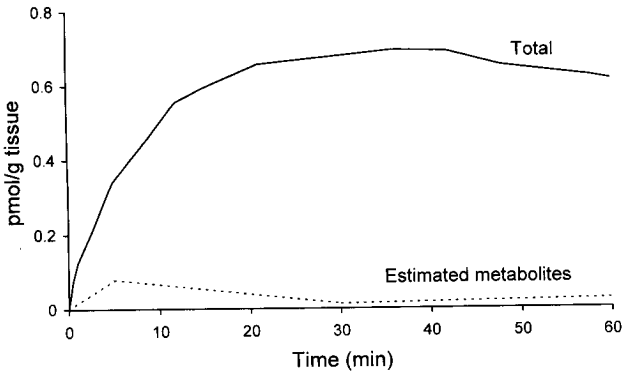

Fig. 6 Measured time-activity curve after injection of [^{11}C]pyrilamine and estimated time-activity curve for labeled metabolites in human brain.

time-activity curve with and without metabolite correction of the input function. An appropriate pattern with a monotonously decreasing function between 10 and 90 min was obtained only when corrections for metabolites were made. Without metabolite correction the impulse response function showed wide oscillations, which is a physiologically meaningless pattern (Fig. 3).

Uptake of [^{11}C]pyrilamine and labeled metabolites in rat brain

Figure 4 shows the time course of [^{11}C]pyrilamine (Fig. 4A) and labeled metabolites (Fig. 4B) in rat brain and plasma. After the [^{11}C]pyrilamine injection, the initial cerebrum (total brain minus cerebellum) uptake was 1.17 ± 0.02%ID/g at 5 min and decreased rapidly to 0.21 ± 0.04%ID/g at 60 min. Plasma radioactivity fell rapidly to a very low level within 5 min after injection. At each time point, the concentration of [^{11}C]pyrilamine in the cerebrum was consistently higher than in the plasma (Fig. 4A). In contrast, the initial uptake of labeled metabolites in the cerebrum was 0.27%ID/g, followed by a rapid decline. At each time point, the concentration of labeled metabolites in the cerebrum was lower than in the plasma (Fig. 4B).

Analysis of labeled metabolites in rat brain

Inspite of the fact that some [^{11}C]pyrilamine metabolites were found to enter the rat brain (Fig. 4B), HPLC of methanol extracted rat brain homogenates at 30, 60 and 90 min after i.v. injection of [^{11}C]pyrilamine showed that less than 1% of the total ^{11}C radioactivity was from metabolites (Fig. 5). This indicates that there was no significant retention of labeled metabolites in rat brain. This result also demonstrates that there is minimal metabolism of [^{11}C]pyrilamine by brain tissue itself.

Estimated metabolite uptake in human brain

An estimated time-activity curve for labeled metabolites of [^{11}C]pyrilamine in human brain, based on the data from the rat experiments and the human PET studies, is shown in Fig. 6 together with a measured time-activity curve after injection of [^{11}C]pyrilamine. In this and the other 6 human brains, no significant amount of metabolites was estimated (1.8 ± 0.3% of total radioactivity at peak [^{11}C]pyrilamine uptake). This metabolite curve represents response to injecting 100% metabolized tracer and it is therefore an overestimation of the actual metabolite concentrations present after injection of [^{11}C]pyrilamine. Therefore, after injection of [^{11}C]pyrilamine the brain radioactivity originating in the metabolites would presumably be negligible.

DISCUSSION

In this study we showed that [^{11}C]pyrilamine is rapidly metabolized, with less than 10% of unmetabolized [^{11}C]pyrilamine remaining in human plasma at 60 min postinjection. Our study also suggests that ^{11}C-labeled metabolites do not significantly accumulate within the cerebral extravascular space.

It has been correctly stipulated[17] that radioligand metabolism affects quantitative parameters obtained with PET. To obtain accurate parameters an exact input function corrected for metabolites is required, so that careful chemical analysis of arterial blood activity has been proposed.[18,19,25] As shown in Fig. 2, after the initial bolus of [^{11}C]pyrilamine the relative concentration of drug metabolites in the plasma increases with time with unmetabolized drug levels significantly smaller than indicated by total plasma activity measurements. Correction of the arterial plasma activities for radioactive metabolites is therefore essential for the quantitative analysis of [^{11}C]pyrilamine binding to histamine H_1 receptors *in vivo*. Furthermore, the extent of [^{11}C]pyrilamine metabolism in the absence and presence of pyrilamine binding

inhibitor (e.g., diphenhydramine or hydroxyzine) was different (data not shown), demonstrating the need to determine metabolites for each study of receptor density by multicompartmental analysis.

Theoretically a labeled metabolite that has a high extraction fraction would be distributed throughout the brain in a manner dependent upon regional blood flow and brain permeability. In this situation correction of the input function for metabolites might not suffice to improve the performance of the tracer kinetic model.[17] Since in humans it is difficult to determine the transfer of metabolites into the brain, data from rodent studies have to suffice to estimate the contribution of metabolites to the total brain radioactivity. In the present study, therefore, the estimation of uptake of [^{11}C]pyrilamine metabolites in human brain was made based on the rat experiments (Fig. 6). This estimation was made assuming that the human brain, like the rat brain, has an initial uptake ratio of [^{11}C]pyrilamine to labeled metabolites of 4.3 (see Fig. 4), and the clearance rate for metabolites from human brain is similar to that from rat brain. Based on these assumptions, no significant amount of metabolites was estimated in human brain. Since these time-activity curves are those estimated when the same activity of [^{11}C]pyrilamine and its labeled metabolites are administered, the brain radioactivity originating in the metabolites will presumably be negligible in images obtained with [^{11}C]pyrilamine. Kinetic analysis of the PET measurements is therefore feasible, and both compartmental and noncompartmental models (such as the impulse response function calculated here) are applicable.

The metabolic stability of the radioligand is another important factor in monitoring receptor-ligand kinetics.[19] In spite of the fact that some [^{11}C]pyrilamine metabolites were found to enter the rat brain (Fig. 4B), from 30 min to 90 min after injection of [^{11}C]pyrilamine less than 1% of the radioactivity in the brain was originating in metabolites of [^{11}C]pyrilamine (Fig. 5). This indicates that there is no significant retention of labeled metabolites in rat brain. Furthermore, this result suggests that there is minimal metabolism of [^{11}C]pyrilamine by brain tissue itself. These results support our estimation in human brain that the metabolites of [^{11}C]pyrilamine do not accumulate within the cerebral extravascular space.

Factor analysis of [^{11}C]pyrilamine PET images of the human brain have shown a relatively high degree of nonspecific binding of the radioligand.[16] The present study indicates that the apparent high nonspecific binding may not be attributed to the tracer metabolism and the entry of the labeled metabolites into the brain. Low density of histamine H_1 receptors in the human brain or other factors, such as lipophilicity of the radioligand or binding to other secondary or non-histamine H_1 receptors, should be considered.

In summary, after intravenous injection [^{11}C]pyrilamine metabolizes in the human body, with only less than 10% of the original radioligand remaining in plasma at 60 min. Rat experiments demonstrated that although metabolites of [^{11}C]pyrilamine may enter the brain, they are not retained for prolonged periods of time. Based on the rat data, the contribution of ^{11}C-labeled metabolites to total [^{11}C]pyrilamine radioactivity in human brain was estimated and found to be negligible. Metabolites of [^{11}C]pyrilamine do not appear to accumulate within the cerebral extravascular space, and there is minimal metabolism of [^{11}C]pyrilamine by brain tissue itself. Therefore, kinetic analysis, with either a compartmental or a noncompartmental model, of the [^{11}C]pyrilamine binding to histamine H_1 receptors would be feasible.

ACKNOWLEDGMENTS

The authors express their gratitudes to John E. Flesher, Marigo Stathis, and Robert C. Smoot for their help in performing the experiments. This work was supported by the U.S.P.H.S. grants NS 30597 and NS 15080.

REFERENCES

1. Lin JS, Sakai K, Jouvet M. Evidence for histaminergic arousal mechanisms in the hypothalamus of cat. *Neuropharmacology* 27: 111–122, 1988.
2. Nicholson AN. Histaminergic systems: daytime alertness and nocturnal sleep. *In* Sleep. Neurotransmitters and Neuromodulators, Wauquier A, Monti JM, Radulovacki M, Gaillard JM (eds.), New York, Raven Press, pp. 211–220, 1985.
3. Wada H, Yamatodani A, Inagaki N, Itowi N, Wang NP, Fukui H. Histaminergic neuron system and its function. *In* Neuroreceptors and Signal Transduction, Kito S, Segawa T, Kuriyama K, Tohyama K, Olsen RW (eds.), New York, Plenum Press, pp. 343–357, 1987.
4. Schwartz JC, Barbin G, Duchemin AM, Garbarg M, Llorens C, Pollard H, et al. Histamine receptors in the brain and their possible functions. *In* Pharmacology of Histamine Receptors, Ganellin CR, Parsons ME (eds.), Bristol, Wright PSG, pp. 351–391, 1982.
5. Hough LB. Cellular localization and possible functions for brain histamine: Recent progress. *Prog Neurobiol* 30: 469–505, 1988.
6. Clark WG, Cumby HR. Biphasic changes in body temperature produced by intracerebroventricular injections of histamine in the cat. *J Physiol* 261: 235–253, 1976.
7. Itowi N, Nagai K, Nakagawa H, Watanabe T, Wada H. Changes in the feeding behavior of rats elicited by histamine infusion. *Physiol Behav* 44: 221–226, 1988.
8. Wada H, Watanabe T, Yamatodani A, Maeyama K, Itoi N, Cacabelos R, et al. Physiological functions of histamine in the brain. *In* Frontiers in Histamine Research, Ganellin CR, Schwartz JC (eds.), Oxford, Pergamon Press, pp. 225–235, 1985.
9. Watanabe T, Taguchi Y, Shiosaka S, Tanaka J, Kubota H, Terano Y, et al. Distribution of the histaminergic neuron system in the central nervous system of rats: A fluorescent immunohistochemical analysis with histidine decarboxylase as a marker. *Brain Res* 295: 13–25, 1984.

10. Tran VT, Chang RSL, Snyder SH. Histamine H-1 receptors identified in mammalian brain membranes with [^{3}H]mepyramine. *Proc Natl Acad Sci USA* 75: 6290–6294, 1978.
11. Chang RSL, Tran VT, Snyder SH. Characteristics of histamine H-1 receptors in peripheral tissues labeled with [^{3}H]mepyramine. *J Pharmacol Exp Ther* 209: 437–442, 1979.
12. Palacios JM, Wamsley JK, Kuhar MJ. The distribution of histamine H-1 receptors in the rat brain: an autoradiographic study. *Neuroscience* 6: 15–37, 1981.
13. Yanai K, Dannals RF, Wilson AA, Ravert HT, Scheffel U, Tanada S, et al. *N*-methyl-[^{11}C]pyrilamine, a radiotracer for histamine H-1 receptors: radiochemical synthesis and biodistribution study in mice. *Nucl Med Biol* 15: 605–610, 1988.
14. Villemagne VL, Dannals RF, Sanchez-Roa PM, Ravert HT, Vazquez S, Wilson AA, et al. Imaging histamine H_1 receptors in the living human brain with ^{11}C-pyrilamine. *J Nucl Med* 32: 308–311, 1991.
15. Yanai K, Watanabe T, Yokoyama H, Hatazawa J, Iwata R, Ishiwata K, et al. Mapping of histamine H_1 receptors in the human brain using [^{11}C]pyrilamine and positron emission tomography. *J Neurochem* 59: 128–136, 1992.
16. Szabo Z, Ravert HT, Gözükara I, Geckle W, Seki C, Sostre S, et al. Noncompartmental and compartmental modeling of the kinetics of carbon-11 labeled pyrilamine in the human brain. *Synapse* 15: 263–275, 1993.
17. Perlmutter JS, Larson KB, Raichle ME, Markham J, Mintun MA, Kilbourn MR, et al. Strategies for *in vivo* measurement of receptor binding using positron emission tomography. *J Cereb Blood Flow Metab* 6: 154–169, 1986.
18. Logan J, Wolf AP, Shiue C-Y, Fowler JS. Kinetic modeling of receptor-ligand binding applied to positron emission tomographic studies with neuroleptic tracers. *J Neurochem* 48: 73–83, 1987.
19. Coenen HH, Wienhard K, Stöcklin G, Laufer P, Hebold I, Pawlik G, et al. PET measurement of D_2 and S_2 receptor binding of 3-*N*-([2′-^{18}F]fluoroethyl)spiperone in baboon brain. *Eur J Nucl Med* 14: 80–87, 1988.
20. Yanai K, Yagi N, Watanabe T, Itoh M, Ishiwata K, Ido T, et al. Specific binding of [^{3}H]pyrilamine to histamine H_1 receptors in guinea pig brain *in vivo*: Determination of binding parameters by a kinetic four-compartment model. *J Neurochem* 55: 409–420, 1990.
21. Huang SC, Phelps ME. Principles of tracer kinetic modeling in positron emission tomography and autoradiography. *In* Positron Emission Tomography and Autoradiography: Principles and applications for the brain and heart, Phelps ME, Mazziotta JC, Schelbert HR (eds.), New York, Raven Press, pp. 287–346, 1986.
22. Szabo Z, Nyitrai L, Sondhaus C. Effects of statistical noise and digital filtering on the parameters calculated from the impulse response function. *Eur J Nucl Med* 13: 148–154, 1987.
23. Van Huffel S, Vandewalle J, De Roo MCh, Willems JL. Reliable and efficient deconvolution technique based on total linear least squares for calculating the renal retention function. *Med Biol Eng Comput* 25: 26–33, 1987.
24. Keyeux A, Ochrymowicz-Bemelmans D, Charlier AA. Induced response to hypercapnia in the two-compartment total cerebral blood volume: influence on brain vascular reserve and flow efficiency. *J Cereb Blood Flow Metab* 15: 1121–1131, 1995.
25. Frost JJ, Douglass KH, Mayberg HS, Dannals RF, Links JM, Wilson AA, et al. Multicompartmental analysis of [^{11}C]carfentanil binding to opiate receptors in humans measured by positron emission tomography. *J Cereb Blood Flow Metab* 9: 398–409, 1989.